Non-linear properties of supercooled liquids in the system Na$_2$O–SiO$_2$

R. Knoche[α], D.B. Dingwell, F.A. Seifert, S.L. Webb

Bayerisches Geoinstitut, Universität Bayreuth, D-95440 Bayreuth, Germany

Abstract

The physical properties, viscosity, density, heat capacity and thermal expansivity, of relaxed supercooled liquids in the temperature range just above the glass transition have been determined for ten compositions along the compositional binary Na$_2$O–SiO$_2$, in the range of 2–45 mole% Na$_2$O, by a combination of scanning calorimetry, dilatometry and micropenetration viscometry. The viscosity, density, heat capacity and thermal expansivity in the glassy state have also been determined.

The heat capacities illustrate a linear composition dependence for the glassy state and a smooth but strongly non-linear composition dependence for the supercooled liquid state. The thermal expansivities were determined by dilatometry up to the glass transition and, by a normalized comparison of relaxation behavior in the glass transition interval, to temperatures ~ 50°C above the glass transition. The expansivity is a linear function of the molar composition in the glass but a strongly non-linear function of molar composition in the supercooled liquid.

The viscosity data just above the glass transition temperature, combined with data from high temperature using the concentric cylinder method, illustrate that the composition dependence of viscosity is strongly non-linear and exhibits an inflection as a function of composition. The glass transition temperature, taken as the peak temperature of the calorimetric measurements, is not in general an isokom in this system.

The data for these property determinations in the Na$_2$O–SiO$_2$ system provide much improved constraints on the partial molar properties of SiO$_2$ liquid and partial molar properties of the SiO$_2$ component in silicate melts. The complex behavior of the transport properties, i.e. the glass transition temperature and the viscosity, point to complexities in viscous flow beyond that of simple binary mixing of the Na$_2$O and SiO$_2$ components.

1. Introduction

The physical properties of silicate glasses and melts are of central importance in material science and geoscience. For an understanding of magmatic processes and the development of general models of igneous petrogenesis the temperature- and pressure-dependent properties of silicate melts are essential.

Under appropriate conditions crystallization may be avoided in many silicate melts down to subliquidus temperatures. Such melts vitrify over a temperature range quite distinct from the crystallization temperature; in a temperature range termed the glass transition (T_g) region. At temperatures just above the glass transition, silicate melts may be studied as supercooled liquids (i.e. liquids that are in local or metastable equilib-

[CA]
[α]*Present address*: Department of Geology, University of Alberta, Edmonton, Alta. T6G 2E3, Canada.

rium) provided the temperatures and time scales of measurement exclude crystallization or liquid–liquid unmixing (Dingwell and Webb, 1990). These low-temperature data can often be determined more precisely than their high-temperature counterparts. Additionally, in combination with high-temperature data for the stable liquid such low-temperature data provide a very wide ($\sim 1000°C$) temperature range over which the behavior of individual properties can be interpolated (Knoche et al., 1992a). Studies of the physical properties of supercooled liquids thus provide a much more complete picture of the temperature- and composition dependence of liquid structure and properties and qualitatively new pictures of the relationship between structure and properties have emerged as a result (Richet, 1984). Finally, the glass transition occurs for dry silicic melts in a temperature range that is relevant to the crystallization of magmatic systems. Thus property determinations near T_g can be applied to the calculation of melt properties during igneous petrogenesis without extrapolation from higher temperature (Dingwell, 1993).

Despite the theoretical advantages of including low-temperature property determinations in the database for the equation of state of silicate melts, a number of practical challenges remain. These challenges have meant that the selection of existing supercooled liquid property data from the literature is difficult (Bansal and Doremus, 1986). For example, the composition dependence of melt transport properties is increasingly sensitive to melt composition at decreasing temperatures. Thus the quality of chemical characterization and purity and homogeneity of samples plays a decisive role in determining the accuracy with which low-temperature data for supercooled liquids can be integrated into the database.

The system $Na_2O–SiO_2$ is a case in point. Although widely separated in composition from either natural melts or those of industrial interest, this system represents a simple model for the variation in melt properties and structure to be expected in natural and industrial melts resulting from a variation in the fraction of the network-forming cation Si. It has accordingly been extensively investigated in both the super- and subliquidus regimes. Data exist in the literature for several physical properties of interest. Despite this and for some of the reasons mentioned above, a number of controversies surround the properties of melts in this simple system. These controversies have implications that go far beyond the simple system. For example, the isothermal composition dependence of viscosity (isokom) may or may not contain inflections. The glass transition temperature (peak temperature) may or may not represent an isokom. The partial molar volumes may or may not be compositionally independent. The expansivity of melts may or may not equal zero in SiO_2-rich compositions, and the heat capacities may or may not be additive. The present investigation of very well-characterized melts in the $Na_2O–SiO_2$ system answers the questions posed by the above statements and in doing so sets the stage for further high-precision studies of the composition dependence of these melt properties.

2. Methods

Ten samples in the $Na_2O–SiO_2$ system were synthesized, one with 98 mole% SiO_2 and the other nine samples ranging from 95 to 55 mole% SiO_2 at intervals of 5 mole%. This compositional range was chosen to avoid synthesis problems for the amounts of material required for the present experiments. Melts with > 45 mole% Na_2O could not be quenched to glasses in sufficient amounts, and melts with < 2 mole% Na_2O have viscosities too high for homogenization.

Starting materials were Na_2CO_3 (99.9%) and SiO_2 (99.995%). The Na_2CO_3 was dried overnight in a vacuum furnace at $220°C$, the SiO_2 powder was weighed in immediately after opening the sealed aluminum package. The chemicals were weighed directly into plastic polyethylene bottles in amounts equivalent to 100 g of decarbonated melt and were roughly homogenized by agitation for ~ 15 min. The mixtures were then melted stepwise into a 75-cm^3 thin-walled Pt crucible at superliquidus temperatures. The products of these fusions were rich in bubbles.

The melts were stirred with a $Pt_{80}Rh_{20}$ spindle until they were homogeneous and bubble free. Finally, the melts were allowed to cool to room temperature at a rate of several degrees per minute. The results were bubble- and crystal-free glasses. The homogeneity of the glasses was checked with the electron microprobe using a 10-μm spot size. Within the spatial resolution of the electron microprobe no inhomogeneity was detected.

Due to the volatility of the Na under the microprobe analytical conditions, the bulk composition of the samples was determined by a separate bulk analytical method, inductively coupled plasma atomic emission spectroscopy (ICP–AES). Water content was determined by Karl–Fischer titration. The results of these analyses are listed in Table 1. The basis for all subsequent calculations and discussions of partial molar properties are the measured compositions of the samples. The analysis of the glasses by Karl–Fischer titration showed an increasing H_2O content with increasing content of Na_2O of the samples. The maximum water content observed was 0.15 wt% in the sample with 45 mole% Na_2O.

Cylinders required for the dilatometer, calorimeter and micropenetration measurements were drilled from the glasses in the Pt crucibles with a diamond corer. For the high-temperature measurements of viscosity and density the rest

Table 1
Chemical composition and water content of the glasses

	(wt%)			(mole%)	
	SiO_2	Na_2O	H_2O	SiO_2	Na_2O
2 mole% Na_2O	98.0	2.0	0.02	98.1	1.9
5 mole% Na_2O	95.0	5.0	0.03	95.1	4.9
10 mole% Na_2O	89.1	10.9	0.05	89.4	10.6
15 mole% Na_2O	83.6	16.4	0.04	84.0	16.0
20 mole% Na_2O	79.3	20.7	0.05	79.8	20.2
25 mole% Na_2O	73.7	26.3	0.03	74.3	25.7
30 mole% Na_2O	68.9	31.1	0.06	69.6	30.4
35 mole% Na_2O	64.0	36.0	0.09	64.7	35.3
40 mole% Na_2O	59.0	41.0	0.10	59.8	40.2
45 mole% Na_2O	54.2	45.8	0.15	55.0	45.0

Analyzed by ICP–AES (average of 2 measurements), water content determined by Karl–Fischer titration.

of the sample was remelted into the crucible used for the measurement at temperatures not higher than the original fusion temperature and stirred again until bubble free. All samples were stored in a desiccator until use in the experiments. After the high-temperature measurements the compositions of the samples were reanalyzed to check for changes in composition due to Na volatilization. No changes in composition could be observed within the error of the ICP–AES measurements.

At the low temperatures of the dilatometric, calorimetric and micropenetration measurements volatilization of Na is not to be expected due to the very high viscosities even at maximum experimental temperatures. During the low-temperature experiments the samples were constantly flushed by an argon gas flow. Thus incorporation of water was not anticipated. To check this assumption the sample with 45 mole% Na_2O was reanalyzed after the low-temperature measurements. This sample with the highest hygroscopy and Na volatility did not show any change in composition or water content. Therefore, the assumption of an unchanged composition of the samples after the low-temperature measurements can be made. None of the samples exhibited crystallization after the dilatometric or calorimetric measurements. For the micropenetration measurements the excursion (the time–temperature path) above the glass transition is somewhat greater than for the scanning calorimetric and dilatometric experiments. Here crystallization occurred for some samples. Only data from samples which did not show any evidence of crystallization during or after the micropenetration experiments were used.

2.1. Heat capacity measurements

The determination of the heat capacity of the glasses and supercooled liquids was performed on glass cylinders with a diameter of 6.4 mm and a length of 10 mm in a differential scanning calorimeter (DSC 111®, Setaram). During the experiments the samples were heated at a constant rate of 5°C min^{-1} up to the relaxed liquid (50–100°C above the glass transition temperature).

Before the measurements the glasses had been cooled with rates of $1°$, $2°$, $5°$ and $10°C$ min^{-1} from the relaxed liquid. As a result, a set of four measurements was obtained for each glass. The calorimeter is calibrated regularly against a cylinder of sapphire with the same dimensions as the samples. The heat capacity data for sapphire were taken from Robie et al. (1979). Based on the measured sapphire heat capacity and the reproducibility of the measured heat capacities for the glasses, the error in the present heat capacity data is $\pm 1\%$.

2.2. Measurements of the molar volume and the thermal expansivity

The density of the glasses at room temperature was determined with the Archimedean buoyancy method in toluene and air. From this and the chemical analyses of the glasses, the molar volume at room temperature was calculated. The measurements were performed on the same glass cylinders used for the dilatometry and calorimetry experiments. Prior to the density measurement these cylinders were cooled from the relaxed liquid with a rate of $5°C$ min^{-1}, permitting an exact comparison of the density data with the expansivity data obtained from the dilatometer and calorimeter data. The density method was calibrated against the densities of Fe, Ir and Pt, yielding an accuracy of $\pm 0.2\%$.

The thermal expansivity of the glasses was measured in a vertical push-rod quartz glass dilatometer (TMA $402®$, Netzsch) in continuous scanning mode on the same cylinders and with the same heating and cooling rates used in the calorimetry experiments. The dilatometer has been calibrated against the thermal expansivity of a sapphire single crystal (NBS sheet 732). This calibration, together with the reproducibility of the measured thermal expansion of the glasses results in an accuracy of $\pm 3\%$ for the molar expansivities.

In the supercooled liquid the expansivity and the molar volume was calculated from the dilatometer trace through the glass transition in combination with the calorimeter trace obtained on exactly the same sample under identical experimental conditions (i.e. same cooling history and same heating rate). This method of calculation for the expansivity of a supercooled liquid at temperatures just above the glass transition is based on the equivalence of the relaxation of enthalpy and volume in the glass transition interval. The theory and applicability of the method are described in detail in Knoche et al. (1992a, b, c) and Webb et al. (1992). The molar expansivities determined by this calculation have a maximum error of $\pm 5\%$.

2.3. Determination of the glass transition temperature

A glass transition temperature (T_g) was determined from the scanning calorimeter and dilatometer curves. These curves show a peak which is characteristic for the glass transition. T_g was assigned to be the peak temperature of the c_p and dV/dT curves. The error in the glass transition temperature, so determined, is $\pm 3°C$ at 1σ based on four measurements each using calorimetry and dilatometry. Different cooling rates lead to a freezing of the structure at different temperatures and therefore to a shift of the glass transition temperature. The influence of the cooling rate on the peak temperature is, however, very small if a constant heating rate is used (e.g., Zallen, 1983).

In this study we used the four different cooling rates principally to check the measurements for their reproducibility and thus increase the precision of the measurements. Although the peak height is influenced strongly by the cooling rate the thermal expansivity of the supercooled liquid should be identical and independent of the cooling rate as the liquid is completely relaxed. This was confirmed by the present measurements.

2.4. Viscosity measurements

The viscosity of the melts was determined using two different techniques. At low temperatures and therefore high viscosities a micropenetration technique was employed (in argon). The micropenetration measurements were per-

formed in the same dilatometer used for the expansivity measurements of the glasses. This technique yields absolute viscosities and has been checked against the viscosity of NBS *711* glass. It has been demonstrated that, over the range of 10^9-10^{11} Pa s, viscosity can be determined with an accuracy of $\pm 0.1 \log_{10}$ Pa s. Details regarding the theory for the micropenetration technique can be found in Dingwell et al. (1992, 1993).

The shear viscosities of the stable liquids at high temperatures were determined using the concentric cylinder technique in equilibrium with air. The furnace, the setup and the computer interface together with the exact procedure and calibration are described by Dingwell and Virgo (1988) and Dingwell (1989a, b, 1990). With this technique a temperature range from 800° to 1650°C and a viscosity range from 10^0 to 10^5 Pa s can be covered. The measured viscosities are relative. The viscometer is regularly calibrated against a standard glass from the U.S. National Bureau of Standards (SRM *711*). The accuracy of the measurements can be determined within $\pm 0.05 \log_{10}$ Pa s. The viscosity of each sample was measured at different temperatures after thermal equilibrium was reached. All observed viscosities were Newtonian, i.e. strain-rate independent.

3. Results and discussion

3.1. Heat capacity

The heat capacities of the glasses and supercooled liquids studied are presented in Fig. 1 and listed in Table 2. Within the accuracy of the measurement the heat capacities of the glasses do not depend on the thermal history (see also Richet and Bottinga, 1986). The peak height changes drastically with changes in the previous cooling rate. The relaxed heat capacities of the supercooled liquids are, as expected, independent of cooling and heating rate. At a common cooling and heating rate the isothermal heat capacities as well as the peak height of the c_p curves increase with increasing Na_2O content of the
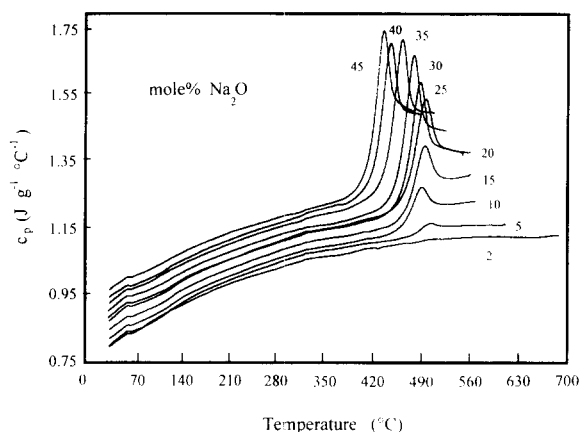

Fig. 1. Heat capacity curves of the glasses and supercooled liquids in the Na_2O-SiO_2 system obtained from scanning calorimetry. The glasses were heated with a rate of 5°C min^{-1} after having previously been cooled from the liquid with 1°C min^{-1}. (The small peak in all curves at ~ 60°C is due to an irregularity in the background measurement.)

samples whereas the peak temperature decreases (Fig. 1).

Up to 400°C all samples studied are still in the glassy state. The isothermal heat capacities measured below this temperature depend linearly on composition in accordance with literature data and models for the heat capacities of glasses (Stebbins et al., 1984; Richet and Bottinga, 1986; Richet, 1987; Fig. 2). At 550°C all samples are in the supercooled liquid state (for the Na-rich samples the heat capacity was extrapolated up to 550°C as the onset of crystallization prevented its measurement up to this temperature). The relaxed isothermal heat capacities show a clearly non-linear dependence on composition (Fig. 2: note that conversion to molar heat capacities does not significantly change this conclusion and that the molar C_p-values are therefore also non-linear).

Available heat capacity data for the Na_2O-SiO_2 system are summarized in Mazurin et al. (1983), Richet et al. (1984), and Bansal and Doremus (1986). The results of the present study are consistent with literature data within the same temperature interval. The differences in heat capacity observed across the glass transition temperature are consistent with the data of Moynihan et al. (1976) and Bershtein et al. (1980).

Table 2
Heat capacity c_p (J g^{-1} °C^{-1}) for the glasses and supercooled melts and glass transition temperature T_g (°C) (cooling rate: 1 °C min^{-1}/heating rate: 5 °C min^{-1})

T (°C)	mole% Na$_2$O									
	2	5	10	15	20	25	30	35	40	45
30	0.76	0.76	0.78	0.81	0.84	0.85	0.87	0.89	0.91	0.93
40	0.78	0.77	0.80	0.83	0.85	0.87	0.89	0.91	0.92	0.95
50	0.80	0.79	0.81	0.84	0.87	0.88	0.90	0.92	0.94	0.96
60	0.81	0.80	0.83	0.85	0.89	0.90	0.92	0.94	0.95	0.97
70	0.81	0.81	0.83	0.86	0.89	0.90	0.92	0.94	0.95	0.98
80	0.82	0.82	0.84	0.87	0.90	0.91	0.93	0.95	0.96	0.99
90	0.83	0.83	0.85	0.88	0.90	0.91	0.94	0.96	0.97	1.00
100	0.85	0.84	0.86	0.88	0.91	0.92	0.94	0.97	0.98	1.01
110	0.86	0.85	0.87	0.90	0.92	0.93	0.95	0.98	0.99	1.02
120	0.87	0.87	0.88	0.91	0.94	0.94	0.97	0.99	1.00	1.03
130	0.88	0.88	0.90	0.92	0.95	0.96	0.98	1.00	1.02	1.04
140	0.89	0.90	0.91	0.94	0.96	0.97	0.99	1.01	1.03	1.05
150	0.90	0.91	0.92	0.95	0.98	0.98	1.00	1.02	1.04	1.06
160	0.91	0.92	0.93	0.96	0.99	0.99	1.01	1.03	1.05	1.07
170	0.92	0.93	0.94	0.97	1.00	1.00	1.02	1.04	1.06	1.08
180	0.93	0.94	0.95	0.98	1.00	1.01	1.03	1.05	1.07	1.09
190	0.94	0.95	0.96	0.98	1.01	1.01	1.04	1.06	1.07	1.10
200	0.95	0.96	0.97	0.99	1.02	1.02	1.04	1.07	1.08	1.10
210	0.95	0.97	0.98	1.00	1.03	1.03	1.05	1.08	1.09	1.11
220	0.96	0.97	0.99	1.01	1.04	1.04	1.06	1.08	1.10	1.12
230	0.97	0.98	0.99	1.01	1.04	1.04	1.07	1.09	1.10	1.13
240	0.98	0.99	1.00	1.02	1.05	1.05	1.07	1.10	1.11	1.14
250	0.98	1.00	1.01	1.03	1.06	1.06	1.08	1.11	1.12	1.14
260	0.99	1.00	1.02	1.04	1.07	1.07	1.09	1.11	1.12	1.15
270	0.99	1.01	1.02	1.05	1.07	1.07	1.10	1.12	1.13	1.16
280	1.00	1.02	1.03	1.05	1.08	1.08	1.10	1.13	1.14	1.16
290	1.01	1.03	1.04	1.06	1.09	1.09	1.11	1.13	1.14	1.17
300	1.01	1.03	1.04	1.07	1.10	1.09	1.11	1.14	1.15	1.17
310	1.02	1.04	1.05	1.07	1.11	1.10	1.12	1.14	1.15	1.18
320	1.03	1.05	1.06	1.08	1.11	1.11	1.13	1.15	1.16	1.18
330	1.03	1.05	1.06	1.09	1.12	1.11	1.13	1.16	1.17	1.18
340	1.04	1.05	1.07	1.09	1.12	1.12	1.14	1.17	1.18	1.19
350	1.04	1.06	1.07	1.09	1.12	1.12	1.14	1.17	1.18	1.19
360	1.04	1.06	1.07	1.10	1.13	1.12	1.14	1.17	1.19	1.20
370	1.04	1.06	1.07	1.10	1.13	1.13	1.14	1.18	1.20	1.20
380	1.05	1.07	1.08	1.10	1.14	1.13	1.15	1.18	1.20	1.22
390	1.05	1.07	1.08	1.11	1.14	1.14	1.16	1.19	1.21	1.23
400	1.06	1.07	1.09	1.11	1.15	1.14	1.16	1.20	1.23	1.26
410	1.06	1.08	1.09	1.12	1.15	1.15	1.17	1.21	1.25	1.31
420	1.06	1.08	1.10	1.12	1.16	1.15	1.18	1.23	1.30	1.41
430	1.06	1.08	1.10	1.12	1.16	1.16	1.19	1.26	1.41	1.64
440	1.07	1.09	1.10	1.13	1.17	1.17	1.20	1.33	1.61	1.70
450	1.07	1.09	1.11	1.14	1.19	1.19	1.24	1.47	1.67	1.54
460	1.08	1.10	1.13	1.16	1.21	1.23	1.32	1.68	1.52	1.51
470	1.08	1.10	1.15	1.19	1.25	1.31	1.49	1.63	1.49	1.50
480	1.08	1.11	1.20	1.25	1.34	1.46	1.66	1.50	1.48	1.49
490	1.09	1.12	1.25	1.35	1.47	1.58	1.52	1.49	1.48	
500	1.09	1.14	1.23	1.37	1.52	1.44	1.45	1.48		
510	1.09	1.14	1.21	1.31	1.42	1.39	1.43	1.48		
520	1.09	1.13	1.20	1.28	1.38	1.37	1.43			

Table 2 (continued)

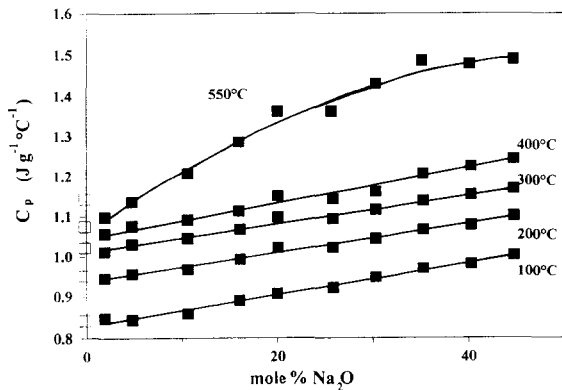| T (°C)	mole% Na₂O									
	2	5	10	15	20	25	30	35	40	45
530	1.10	1.13	1.20	1.28	1.37	1.37				
540	1.10	1.13	1.20	1.28	1.36	1.36				
550	1.10	1.14	1.20	1.28	1.36	1.36				
560	1.10	1.14	1.20	1.28	1.36					
570	1.10	1.14								
580	1.10	1.14								
590	1.10	1.14								
600	1.10	1.14								
610	1.10	1.14								
620	1.10									
630	1.10									
640	1.10									
650	1.10									
660	1.10									
670	1.10									
680	1.10									
T_g (c_p)	506	505	492	497	497	490	481	464	447	437
T_g (dV/dT)	506	502	495	498	495	489	478	463	447	436

Fig. 2. Isothermal heat capacities of the glasses (100°, 200°, 300°, 400°C) and supercooled melts (550°C — for the Na-rich samples the heat capacity was extrapolated up to 550°C as the onset of crystallization prevented its measurement up to this temperature). The errors are less than the size of the symbols. The data for SiO₂ (Table 3) are also plotted.

The non-linear composition dependence of the heat capacity of the supercooled liquids indicates that multi-linear fits of heat capacity will have only limited success in predicting the thermal properties of such systems.

3.2. Molar volume and thermal expansivity

3.2.1. Molar volume at room temperature

The glass densities at room temperature (Table 4 and volumes in Fig. 3) increase non-linearly with increasing Na₂O. The density of glasses in this system has been studied extensively (Mazurin et al., 1983). Bansal and Doremus (1986) determined mean values for the densities from 15 different studies. These values are in good agreement with our data though our data are consistently higher, generally by ~0.2%. An explanation can be found in the fact that, in the reported studies, melts were generally quenched by pouring them onto a steel plate. This corresponds to a cooling rate for the glasses of some 10–100°C min⁻¹. In our study we cooled the glasses with 5°C min⁻¹ from the liquid state before the determination of density. Therefore, the higher density of the present glasses could result from their lower fictive temperature. (Based on the data presented in Table 7, an order of magnitude increase in quench rate results in ≤0.15% decrease in density.)

Table 3
Literature data for SiO_2 glass and melt used in the present calculations

Parameter		Value	Reference[a]
T_g (°C)		1,207	[1]
c_p	100°C	0.838	[2]
(J g^{-1} °C^{-1})		0.840	[1]
		0.840	[3]
	200°C	0.974	[2]
		0.944	[1]
		0.950	[3]
	300°C	1.046	[2]
		1.018	[1]
		1.025	[3]
	400°C	1.089	[2]
		1.073	[1]
		1.072	[3]
	550°C	1.129	[2]
		1.131	[1]
		1.137	[3]
Density (g cm^{-3})	20°C	2.20	[3]
Molar volume	1,100°C	27.3	[4]
(cm^3 mol^{-1})	1,400°C	26.9	[5]
dV/dT	100°C	0.04	[3]
(10^{-4} cm^3 mol^{-1} °C^{-1})	400°C	0.05	
	520°C	0.05	
Viscosity	1,000°C	15.80	[3]
(log$_{10}$ η, η in Pa s)	1,200°C	11.82	
	1,400°C	8.80	
	1,600°C	7.12	

[a]*References*: [1] = Richet and Bottinga (1984); [2] = Robie et al. (1979); [3] = Bansal and Doremus (1986); [4] = Brückner (1970); [5] = Lange and Carmichael (1990).

Table 4
Density of the glasses at 19.8°C

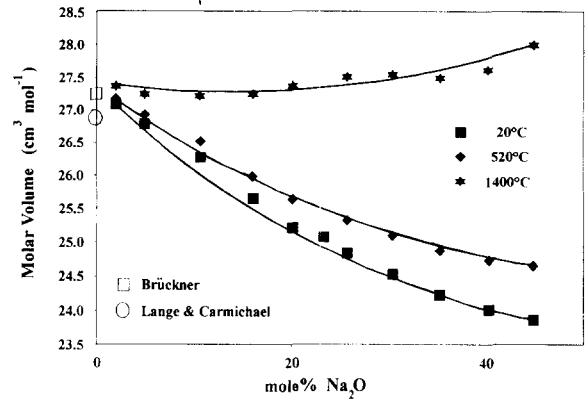| Na_2O content (mole%)	ρ (g cm^{-3})	Na_2O content (mole%)	ρ (g cm^{-3})
2	2.220	25	2.439
5	2.247	30	2.473
10	2.295	35	2.507
15	2.354	40	2.534
20	2.398	45	2.554

Densities ±0.2% at 1σ.

Fig. 3. Molar volumes of the glasses (20°C), supercooled melts (520°C) and stable melts (1400°C). The errors are the size of the *symbols*. The data for SiO_2 are also plotted.

3.2.2. Thermal expansion of the glasses and supercooled liquids

The thermal expansion of the glasses measured in the dilatometer is linearly dependent on temperature. The molar volume of the glasses up to the glass transition (Table 5) can be described as a second-order polynomial using the room temperature density and the glassy expansivity data (Table 6). Our data for the expansion of the glasses are comparable to the literature data [for a summary, see Mazurin et al. (1983)]. Systematic studies of thermal expansion over a wide range of compositions are reported by Samsoen (1926, 1928), Turner and Winks (1930), and Shelby (1976). Their data are in excellent agreement with ours.

In the supercooled liquid the thermal expansion and the molar volume were determined from the combination of calorimetry and dilatometry (Table 7). The thermal expansivity increases non-linearly with increasing Na_2O (Fig. 4; to enable an isothermal comparison the expansivities of the samples rich in Na are extrapolated in temperature). The continuous increase is interrupted by the data point at 10 mole% Na_2O. This deviation lies outside of the error of the measurements. A satisfactory explanation for this cannot be given though it is worth noting that the same sample also shows a deviation in the glass transition temperature.

Some authors also give values for the thermal

Table 5
Molar volume ($cm^3 mol^{-1}$) for the glasses and supercooled melts (cooling rate: $1°C min^{-1}$/heating rate: $5°C min^{-1}$)

T (°C)	mole % Na_2O									
	2	5	10	15	20	25	30	35	40	45
30	27.08	26.78	26.26	25.65	25.22	24.84	24.53	24.24	24.02	23.87
40	27.09	26.78	26.26	25.66	25.23	24.84	24.54	24.25	24.02	23.88
50	27.09	26.79	26.27	25.66	25.24	24.85	24.55	24.25	24.03	23.89
60	27.09	26.79	26.27	25.67	25.24	24.86	24.56	24.26	24.04	23.90
70	27.09	26.79	26.28	25.67	25.25	24.87	24.57	24.28	24.05	23.91
80	27.09	26.79	26.28	25.68	25.26	24.89	24.58	24.29	24.06	23.93
90	27.09	26.80	26.29	25.69	25.27	24.89	24.59	24.30	24.08	29.94
100	27.10	26.80	26.29	25.69	25.28	24.90	24.60	24.31	24.09	23.95
110	27.10	26.80	26.30	25.70	25.29	24.91	24.61	24.32	24.10	23.96
120	27.10	26.80	26.30	25.71	25.29	24.92	24.62	24.33	24.11	23.98
130	27.10	26.81	26.31	25.72	25.30	24.93	24.63	24.34	24.13	23.99
140	27.10	26.81	26.31	25.72	25.31	24.94	24.64	24.35	24.14	24.00
150	27.11	26.81	26.32	25.73	25.32	24.95	24.65	24.36	24.15	24.02
160	27.11	26.82	26.32	25.73	25.32	24.96	24.66	24.38	24.17	24.03
170	27.11	26.82	26.33	25.74	25.33	24.97	24.67	24.39	24.18	24.04
180	27.11	26.82	26.33	25.75	25.34	24.98	24.68	24.40	24.19	24.06
190	27.11	26.83	26.34	25.76	25.35	24.99	24.69	24.41	24.21	24.07
200	27.12	26.83	26.34	25.76	25.36	25.00	24.70	24.43	24.22	24.09
210	27.12	26.83	26.35	25.77	25.37	25.01	24.71	24.44	24.23	24.10
220	27.12	26.84	26.35	25.78	25.38	25.02	24.73	24.45	24.25	24.12
230	27.12	26.84	26.36	25.78	25.39	25.03	24.74	24.46	24.26	24.13
240	27.12	26.84	26.37	25.79	25.40	25.04	24.75	24.48	24.28	24.15
250	27.13	26.85	26.37	25.80	25.41	25.05	24.76	24.49	24.29	24.16
260	27.13	26.85	26.38	25.81	25.41	25.06	24.77	24.50	24.31	24.18
270	27.13	26.85	26.38	25.81	25.42	25.07	24.78	24.51	24.32	24.19
280	27.14	26.86	26.39	25.82	25.43	25.08	24.79	24.53	24.34	24.21
290	27.14	26.86	26.39	25.83	25.44	25.09	24.81	24.54	24.35	24.23
300	27.14	26.86	26.40	25.84	25.45	25.10	24.82	24.56	24.37	24.24
310	27.14	26.87	26.40	25.85	25.46	25.11	24.83	24.57	24.38	24.26
320	27.14	26.87	26.41	25.85	25.47	25.12	24.84	24.58	24.40	24.27
330	27.15	26.87	26.41	25.86	25.48	25.13	24.86	24.60	24.41	24.29
340	27.15	26.88	26.42	25.87	25.49	25.14	24.87	24.61	24.43	24.31
350	27.15	26.88	26.42	25.88	25.50	25.15	24.88	24.63	24.44	24.33
360	27.15	26.88	26.43	25.89	25.51	25.16	24.89	24.64	24.46	24.34
370	27.15	26.89	26.43	25.90	25.52	25.17	24.90	24.65	24.48	24.36
380	27.15	26.89	26.44	25.90	25.53	25.18	24.92	24.67	24.49	24.38
390	27.16	26.89	26.45	25.91	25.54	25.19	24.93	24.68	24.51	24.39
400	27.16	26.90	26.45	25.92	25.55	25.20	24.94	24.70	24.53	24.41
410	27.16	26.90	26.46	25.93	25.56	25.22	24.96	24.72	24.55	24.43
420	27.17	26.90	26.46	25.94	25.57	25.23	24.97	24.73	24.57	24.46
430	27.17	26.91	26.47	25.95	25.58	25.24	24.98	24.75	24.59	24.49
440	27.17	26.91	26.47	25.96	25.59	25.25	25.00	24.77	24.62	24.53
450	27.17	26.91	26.48	25.96	25.60	25.26	25.02	24.79	24.66	24.58
460	27.18	26.92	26.49	25.97	25.61	25.28	25.04	24.82	24.70	
470	27.18	26.92	26.49	25.99	25.62	25.30	25.06	24.86		
480	27.18	26.93	26.50	26.00	25.64	25.32	25.10	24.89		
490	27.19	26.93	26.51	26.02	25.66	25.36	25.14			
500	27.19	26.94	26.53	26.04	25.70	25.39				
510	27.19	26.94	26.54	26.06	25.72	25.42				
520	27.19	26.95	26.55	26.08	25.74					
530	27.20	26.95	26.56	26.10						

Table 5 (continued)

T (°C)	mole % Na$_2$O									
	2	5	10	15	20	25	30	35	40	45
540	27.20	26.96	26.57							
550	27.20	26.96	26.58							
560	27.21	26.97								
570	27.21	26.97								
580	27.22	26.98								
590	27.22	26.98								
600	27.22									
610	27.23									
620	27.23									
630	27.23									
640	27.23									
650	27.23									
660	27.24									
670	27.24									
680	27.24									

Table 6
Molar volume (cm^3 mol^{-1}) of the glasses as a function of temperature:

$$V \ (\text{cm}^3\text{mol}^{-1}) = a + b \cdot 10^{-4} T + c \cdot 10^{-7} T^2, \quad \text{with } T = \text{temperature } (°C)$$

	a	b	c	T (°C)	Molar weight (g mol^{-1})
2 mole% Na$_2$O	27.08	1.43	1.20	20–440	60.121
5 mole% Na$_2$O	26.77	2.76	1.33	20–420	60.176
10 mole% Na$_2$O	26.26	4.67	1.19	20–420	60.285
15 mole% Na$_2$O	25.64	6.03	2.71	20–420	60.386
20 mole% Na$_2$O	25.20	7.40	3.85	20–420	60.464
25 mole% Na$_2$O	24.82	8.48	3.51	20–410	60.570
30 mole% Na$_2$O	24.51	9.18	5.27	20–400	60.660
35 mole% Na$_2$O	24.21	10.17	5.63	20–390	60.751
40 mole% Na$_2$O	23.99	10.46	7.39	20–370	60.845
45 mole% Na$_2$O	23.84	10.80	8.80	20–360	60.934

Cooling-rate/heating-rate: 5°C min^{-1}/5°C min^{-1}.

expansivity of the supercooled liquids above the glass transition. Those data have been obtained by determining the slope of the dL curve in the inflection point above the beginning of the glass transition interval (the equivalent of using "peak" values, the thermal expansivity at the maximum of the dV/dT curve; see also Knoche et al., 1992a). This explains the overestimates of the expansivity in the data from Samsoen (1926, 1928), Amrhein (1963), and Suzuki and Abe (1981). In contrast to this, Turner and Winks (1930) and Maklad and Kreidl (1971) report a thermal expansivity above T_g which is clearly much too low. This is most likely due to too large a force being exerted on the sample during the measurement, resulting in appreciable viscous deformation under the applied load in the glass transition interval.

The thermal expansivities of the supercooled liquids illustrated in Fig. 4 can be used to extrapolate from 98% to 100% SiO$_2$. The resulting expansivity of SiO$_2$ liquid is extremely small, within error of zero. This estimate of the relaxed, low-temperature expansivity of SiO$_2$ compares with

Table 7
Calculated dV/dT and α_V [$= (1/V)\cdot(dV/dT)$] from the comparison of the calorimetry and dilatometry data, together with the molar volume of the supercooled melts at temperature T

	dV/dT (10^{-4} cm^3 mol^{-1} °C^{-1})	α_V (10^{-6} °C^{-1})	V (cm^3 mol^{-1})	T (°C)
2 mole% Na$_2$O	4.0 ± 1.0	14.6 ± 2.9	27.179 ± 0.010	560
5 mole% Na$_2$O	5.0 ± 0.5	18.6 ± 1.9	26.948 ± 0.003	560
10 mole% Na$_2$O	10.1 ± 0.4	38.0 ± 1.5	26.531 ± 0.004	540
15 mole% Na$_2$O	18.1 ± 0.7	69.6 ± 2.7	26.026 ± 0.003	540
20 mole% Na$_2$O	22.5 ± 1.0	87.6 ± 4.0	25.686 ± 0.004	540
25 mole% Na$_2$O	24.6 ± 0.7	97.1 ± 2.7	25.346 ± 0.001	530
30 mole% Na$_2$O	26.9 ± 0.9	107.3 ± 3.8	25.092 ± 0.004	520
35 mole% Na$_2$O	30.1 ± 0.6	121.0 ± 2.4	24.840 ± 0.003	510
40 mole% Na$_2$O	31.0 ± 0.7	125.7 ± 3.0	24.639 ± 0.002	490
45 mole% Na$_2$O	34.2 ± 1.6	139.5 ± 6.7	24.512 ± 0.010	480
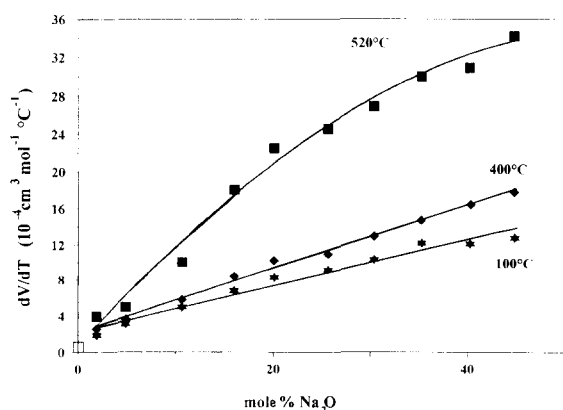
Fig. 4. Isothermal molar expansivities of the glasses (100°, 400°C) and melts (520°C). The errors are less than the size of the *symbols*. The data for SiO$_2$ (see Table 3) are also plotted.

the low expansivity measured for SiO$_2$ glass in this temperature range (Brückner, 1970). These results, taken together, imply that the glass transition in SiO$_2$ will impart a very small expansivity change to the melt. The generally small expansivity of SiO$_2$ indicated in Fig. 4 is similar to the result of multi-component fits of silicate melt densities as well (Bottinga and Weill, 1970; Lange and Carmichael, 1990). It is worth pointing out, however, that the non-linear composition dependence of the thermal expansivity in this system implies a higher effective expansivity of the SiO$_2$ component in the silicate melt structure. This excess behavior of the expansivity is

observed for the first time in this study. One might interpret the non-linear composition dependence of expansivity in terms of a fundamental difference in the expansivity of SiO$_4$ tetrahedra that are fully polymerized vs. those which have non-bridging oxygens. The proposal by Bockris et al. (1956) that the expansivity of SiO$_2$-rich silicate melts on this (and other) joins goes through zero and becomes negative with increasing SiO$_2$ content appears is refuted by the present data.

3.3. Viscosity

The data for the viscosity of the melts are listed in Table 8. Not all of the ten samples could be studied with the micropenetration and/or the concentric cylinder technique. The surface of the samples with 2, 5 and 10 mole% Na$_2$O began to crystallize during the micropenetration experiments. For the samples with 2 and 5 mole% Na$_2$O the viscosity at the maximum experimental temperatures was still too high to allow equilibrium measurements. Therefore, only for compositions with 15–45 mole% Na$_2$O could low- and high-temperature viscosities be determined.

Non-Arrhenian behavior was observed for all compositions studied. The low-temperature viscosity data, together with the high-temperature viscosity data, were fit within error to a second-order polynomial (Table 9; Fig. 5). Arrhenian behavior is reported in the literature for the vis-

Table 8
Viscosity of the melts

	T (°C)	$\log_{10} \eta$ (η in Pa s)		T (°C)	$\log_{10} \eta$ (η in Pa s)		T (°C)	$\log_{10} \eta$ (η in Pa s)
5 mole% Na$_2$O	1,575	2.24	25 mole% Na$_2$O	494.4	10.73	40 mole% Na$_2$O	444.5	10.83
	1,600	2.18		502.6	10.29		454.2	10.40
	1,625	2.09		509.2	9.98		464.0	9.94
	1,650	2.01		519.0	9.69		474.5	9.52
	1,675	1.94		533.7	9.28		484.1	9.20
				543.5	8.94		1,000	1.57
10 mole% Na$_2$O	1,500	1.77		1,200	1.53		1,050	1.37
	1,550	1.60		1,250	1.37		1,100	1.11
	1,600	1.43		1,300	1.21		1,150	0.93
	1,650	1.28		1,350	1.05		1,200	0.72
				1,400	0.91		1,250	0.57
15 mole% Na$_2$O	523.9	11.05		1,450	0.79		1,300	0.38
	542.9	10.57						
	582.5	9.53	30 mole% Na$_2$O	474.1	11.08	45 mole% Na$_2$O	433.2	10.76
	1,350	1.77		489.0	10.42		444.1	10.22
	1,400	1.59		504.4	9.86		454.0	9.73
	1,450	1.42		514.4	9.35		463.6	9.30
	1,500	1.28		1,050	1.99		1,100	0.65
	1,600	1.00		1,100	1.76		1,125	0.56
				1,150	1.52		1,150	0.40
20 mole% Na$_2$O	504.3	10.63		1,200	1.32		1,175	0.34
	518.9	10.41		1,250	1.14		1,200	0.25
	533.4	9.90		1,300	0.98		1,225	0.16
	548.5	9.38		1,350	0.83		1,250	0.08
	1,250	1.70						
	1,300	1.49	35 mole% Na$_2$O	464.0	10.78			
	1,350	1.32		474.4	10.27			
	1,400	1.17		484.0	9.85			
	1,450	1.03		493.9	9.51			
	1,500	0.90		503.9	9.16			
				1,050	1.72			
				1,100	1.47			
				1,150	1.32			
				1,200	1.05			
				1,250	0.93			
				1,300	0.73			
				1,350	0.58			

Viscosity $\pm 15\%$ ($\pm 0.10 \log_{10}$) from 10^9 to 10^{11} Pa s. Viscosity $\pm 5\%$ ($\pm 0.05 \log_{10}$) from 10^0 to 10^5 Pa s.

cosity of SiO$_2$ melt (e.g., Richet, 1984). In Fig. 5 it can be seen that the curvature of the non-Arrhenian curves decreases with increasing SiO$_2$ content.

In an isothermal plot of the viscosities as a function of composition (Fig. 6) an inflection point can be seen at all temperatures. As this inflection point occurs consistently at all temperatures, i.e. is obtained from high-temperature measurements as well as from low-temperature measurements, we can exclude the possibility that it is an experimental artifact. The inflection point generally occurs at a composition around 30 mole% Na$_2$O with exception of the 500°C isotherm where the inflection point lies at ~ 25 mole% Na$_2$O. The numerical description of the isothermal viscosities with a polynomial of third order (i.e. with an inflection point) can be jus-

Table 9
Viscosity as a function of temperature:

$\log_{10} \eta$ (η in Pa s) $= a + bx + cx^2$, with $x = 10^4/T$ and T in K

	a	b	c
2 mole% Na$_2$O	–	–	–
5 mole% Na$_2$O	– 3.646	1.089	–
10 mole% Na$_2$O	– 4.506	1.112	–
15 mole% Na$_2$O	– 2.027	0.209	0.067
20 mole% Na$_2$O	– 1.152	– 0.077	0.078
25 mole% Na$_2$O	0.794	– 0.595	0.103
30 mole% Na$_2$O	1.173	– 0.712	0.108
35 mole% Na$_2$O	0.562	– 0.596	0.099
40 mole% Na$_2$O	0.565	– 0.648	0.099
45 mole% Na$_2$O	1.207	– 0.883	0.110
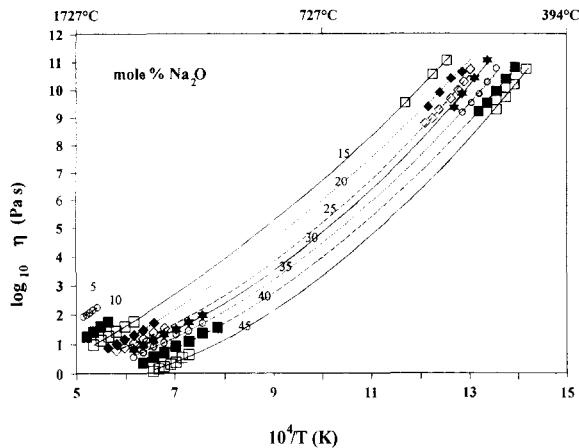
Fig. 5. Plot of melt viscosities in the Na$_2$O–SiO$_2$ system. The low-temperature data from micropenetration measurements (10^9–10^{11} Pa s) can be combined with the high-temperature, concentric cylinder data (10^0–10^3 Pa s) through a second-order polynomial within the error of the methods. This implies a non-Arrhenian behavior for all the samples studied. Errors are less than the size of the symbols. (Complete data sets could not be obtained for all compositions. See explanation in the text.)
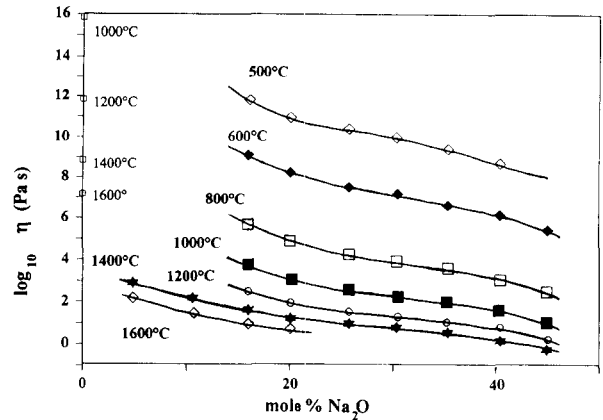

Fig. 6. Isothermal viscosities of the melts from both micropenetration and concentric cylinder determinations. The data for SiO$_2$ (see Table 3) are also plotted. The errors are everywhere less than the size of the symbols.

tified from the number and quality of data available. For an exact location of the inflection point more data points are required. An influence of the immiscibility gap in the system can be ruled out as this gap occurs at compositions much poorer in Na$_2$O (Haller et al., 1974).

The viscosities of melts in the Na$_2$O–SiO$_2$ system have been studied extensively [see summary in Mazurin et al. (1983) and Bansal and

Doremus (1986)]. The low, superliquidus viscosities have been determined by many authors in relatively good agreement. In contrast, low-temperature viscosities are less well known and the results of different investigations differ by up to an order of magnitude.

This is also the case in the present study where our high-temperature superliquidus viscosities are in very good agreement with the data from the literature but our low-temperature data are not. This is partly due to the fact that all low-temperature methods for the determination of viscosity have in the past contained a larger error than those for high temperatures. Slight differences in composition (in Na content and in minor-element content) also affect the low-temperature viscosities more than the high-temperature viscosities. A subtle inflection in the composition dependence of viscosity exists at all temperatures of comparison. This inflection leads to a deviation of viscosity at higher Na$_2$O contents up to more than a $\log_{10}$ unit less that would be predicted from the SiO$_2$-rich melt trend. The observed inflection persists from 500° to 1600°C in the range of 20–30 mole% Na$_2$O. It is clear evidence that viscosities on the Na$_2$O–SiO$_2$ join must be explained by a structural model more complex than a simple mixing of bridging and non-bridging oxygens and may presumably in-

dicate the direct influence of the distribution of Q species on the nature of viscous flow.

3.4. Glass transition temperatures

The glass transition temperatures T_g determined from the calorimeter and dilatometer curves are listed in Table 2 (Fig. 7). An overview over the existing literature data for T_g in the system Na_2O-SiO_2 can be found in Mazurin et al. (1983). The T_g data given by different authors differ greatly. Part of the explanation lies in the different thermal histories of the samples, part in the differing experimental techniques (not properties!) used for T_g determination and part in differing definitions for T_g. Thus, a comparison of the data is not possible. Some authors have, however, determined the compositional dependence of the glass transition temperature over a wide range of compositions (including low Na_2O contents) systematically (e.g., Samsoen, 1926, 1928; Turner and Winks, 1930; Shelby, 1976). Especially at low Na_2O contents, the compositional dependence of T_g is not clear from the literature. Some authors report a continuous increase of T_g with increasing SiO_2 content (Maklad and Kreidl, 1971), others report local minima at differing Na contents (Turner and Winks, 1930, at 10 mole% Na_2O; Samsoen, 1926, 1928, at ~ 25 mole% Na_2O) others observe a decrease of T_g with decreasing Na_2O content after
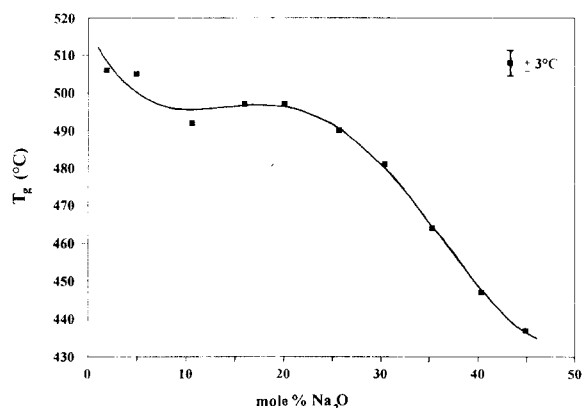
reaching a maximum value at ~ 15 mole% Na_2O (Mazurin et al., 1970; Shelby, 1976).

The T_g data determined in this study compare qualitatively quite well with the systematic determinations from Turner and Winks (1930), and Shelby (1976). A quantitative comparison to the literature data is not appropriate because the measured T_g depends upon both the experimental parameters and the chosen definition of T_g. Our data appear to confirm the existence of a local minimum in T_g at ~ 10 mole% Na_2O. Even if the sample with 10 mole% Na_2O was partially phase separated an influence of the miscibility gap which occurs at around the same composition (Haller et al., 1974) would not lead to the occurrence of such a minimum. The calorimetrically measured peak temperature does not represent an isokom, a line of constant viscosity. This non-equivalence does not, however, mean that the enthalpic and shear relaxation times of the melts are not equivalent. There are two reasons for this.

(1) The peak temperature is a rough approximation to a constant value of enthalpic relaxation time. In detail, the location of the peak temperature depends on thermal history. The calorimetric measurements are non-linear relaxation measurements on glasses with thermal histories. The existence of the peak is a consequence of mismatch between the fictive temperature of the sample and the glass transition temperature associated with the subsequent heating rate.

(2) The shear relaxation time is not exactly proportional to viscosity, rather it is related through the Maxwell equation by the shear modulus at the temperature of the glass transition.

Thus the shear and enthalpic relaxation times may still be equivalent although the comparison of peak temperature and viscosity does not yield an isokom.

4. Summary

These high-precision determinations of the physical properties of supercooled liquids in the Na_2O-SiO_2 system have revealed several impor-

Fig. 7. Glass transition temperatures of the melts in the Na_2O-SiO_2 system.

tant details of the composition- and temperature dependence of melt properties. Volume, thermal expansivity and heat capacity of supercooled liquids in the Na_2O-SiO_2 system are all strongly non-linear functions of composition. The extrapolated values of the partial molar properties of SiO_2 confirm anomalous properties for this composition in the supercooled liquid (relaxed) state. Isokoms of the system exhibit an inflection between 20 and 30 mole% Na_2O that persists over a 1000°C temperature range. The glass transition temperature also exhibits an inflection, at high SiO_2 contents. The peak temperatures from scanning calorimetry and dilatometry although identical do not represent an isokom.

Acknowledgements

References

Amrhein, E.-M., 1963. Das dielektrische Verhalten binärer Oxydgläser im Mikrowellengebiet zwischen 100 und 900°C. Glastech. Ber., 36: 425-444.

Bansal, N.P. and Doremus, R.H., 1986. Handbook of Glass Properties. Academic Press, Orlando, Fla., 680 pp.

Bershtein, V.A., Egorov, V.M., Emelyanov, Y.A., Kelina, R.P., Stepanov, V.A. and Cherkas, G.D., 1980. Fiz. Khim. Stekla, 6: 289-299. [In: O.V. Mazurin, M.V. Streltsina and T.P. Shvaiko-Shvaikovskaya (Editors), Handbook of Glass Data, Part A. Elsevier, Amsterdam, 669 pp. (1983).]

Bockris, J.O'M., Tomlinson, J.W. and White, J.L., 1956. The structure of the liquid silicates: partial molar volumes and expansivities. Trans. Faraday Soc., 52: 299-310.

Bottinga, Y. and Weill, D.F., 1970. Density of liquid silicate systems calculated from partial molar volumes of oxide components. Am. J. Sci., 269: 169-182.

Brückner, R., 1970. Properties and structure of vitreous silica, I. J. Non-Cryst. Solids, 5: 123-175.

Dingwell, D.B., 1989a. Effect of fluorine on the viscosity of diopside liquid. Am. Mineral., 74: 333-338.

Dingwell, D.B., 1989b. Shear viscosities of ferrosilicate liquids. Am. Mineral., 74: 1038-1044.

Dingwell, D.B., 1990. Shear viscosities of galliosilicate liquids. Am. Mineral., 75: 1231-1237.

Dingwell, D.B., 1993. Experimental strategies for the determination of granitic melt properties at low temperature. In: J.L.R. Touret and A.B. Thompson (Guest-Editors), Fluid-Rock Interaction in the Deeper Continental Lithosphere. Chem. Geol., 108: 19-30 (special issue).

Dingwell, D.B. and Virgo, D., 1988. Viscosities of melts in the $Na_2O-FeO-Fe_2O_3-SiO_2$ system and factors controlling the relative viscosities of fully polymerized silicate melts. Geochim. Cosmochim. Acta, 52: 395-403.

Dingwell, D.B. and Webb, S.L., 1990. Relaxation in silicate melts. Eur. J. Mineral., 2: 427-449.

Dingwell, D.B., Knoche, R., Webb, S.L. and Pichavant, M., 1992. The effect of B_2O_3 on the viscosity of haplogranitic liquids. Am. Mineral., 77: 457-461.

Dingwell, D.B., Knoche, R. and Webb, S.L., 1993. The effect of P_2O_5 on the viscosity of haplogranitic liquid. Eur. J. Mineral., 5: 133-140.

Haller, W., Blackburn, D.H. and Simmons, J.H., 1974. Miscibility gaps in alkali-silicate binaries — data and thermodynamic interpretation. J. Am. Ceram. Soc., 57: 120-126.

Knoche, R., Dingwell, D.B. and Webb, S.L., 1992a. Temperature-dependent thermal expansivities of silicate melts: the system anorthite-diopside. Geochim. Cosmochim. Acta, 56: 689-699.

Knoche, R., Dingwell, D.B. and Webb, S.L., 1992b. Non-linear temperature dependence of liquid volumes in the system albite-anorthite-diopside. Contrib. Mineral. Petrol., 111: 61-73.

Knoche, R., Webb, S.L. and Dingwell, D.B., 1992c. A partial molar volume for B_2O_3 in haplogranitic melt. Can. Mineral., 30: 561-569.

Lange, R.A. and Carmichael, I.S.E., 1990. Thermodynamic properties of silicate liquids with emphasis on density, thermal expansion and compressibility. Rev. Mineral., 24: 25-64.

Maklad, M.S. and Kreidl, N.J., 1971. Some effects of OH groups on sodium silicate glasses. In: Proceedings of the 9th International Congress on Glass, Vol. 1, Versailles, pp. 75-100.

Mazurin, O.V., Roskova, G.P. and Kluyev, V.P., 1970. Properties of phase-separated soda-silica glasses as a means of investigation of their structure. Discuss. Faraday Soc., 50: 191-199.

Mazurin, O.V., Streltsina, M.V. and Shvaiko-Shvaikovskaya, T.P., 1983. Handbook of Glass Data, Part A. Silica Glass and Binary Silicate Glasses. Elsevier, Amsterdam, 669 pp.

Moynihan, C.T., Easteal, A.J., Tran, D.C., Wilder, J.A. and Donovan, E.P., 1976. Heat capacity and structure relaxation of mixed-alkali glasses. J. Am. Ceram. Soc., 59: 137-140.

Richet, P., 1984. Viscosity and configurational entropy of silicate melts. Geochim. Cosmochim. Acta, 48: 471-483.

Richet, P., 1987. Heat capacity of silicate glasses. In: Y. Bottinga and J.-C. Mathieu (Guest-Editors), Liquid Sili-

cates. Chem. Geol., 62: 111-124 (special issue).

Richet, P. and Bottinga, Y., 1984. Glass transitions and thermodynamic properties of amorphous SiO_2, $NaAlSi_nO_{2n+2}$ and $KAlSi_3O_8$. Geochim Cosmochim Acta, 48: 453-470.

Richet, P. and Bottinga, Y., 1986. Thermochemical properties of silicate glasses and liquids: a review. Rev. Geophys., 24: 1-25.

Richet, P., Bottinga, Y. and Tequi, C., 1984. Heat capacity of sodium silicate liquids. Comm. Am. Ceram. Soc., 67: C6-C8.

Robie, R.A., Hemingway, B.S. and Fisher, J.R., 1979. Thermodynamic Properties of Minerals and Related Substances at 298.15 K and 1 bar (10^5 Pascals) Pressure and at Higher Temperatures. U.S. Gov. Print. Off., Washington, D.C., 456 pp.

Samsoen, M.-O., 1926. Sur l'étude dilatométrique et thermique des verres composés de silice et de soude. C.R. Acad. Sci. Paris, 183: 285-286.

Samsoen, M.-O., 1928. Contribution a l'étude de l'état vitreux et de la dilatation des verres. Ann. Phys., Sér., 10: 35-127.

Shelby, J.E., 1976. Thermal expansion of mixed-alkali silicate glasses. J. Appl. Phys., 47: 4489-4496.

Stebbins, J.F., Carmichael, I.S.E. and Moret, L.K., 1984. Heat capacities and entropies of silicate liquids and glasses. Contrib. Mineral. Petrol, 86: 131-148.

Suzuki, S. and Abe, Y., 1981. The free volume of some oxide glasses at the transition temperature. J. Non-Cryst. Solids, 43: 141-143.

Turner, W.E.S. and Winks, F., 1930. The thermal expansion of glass, Part II. Glasses of the series sodium metasilicate-silica. J. Soc. Glass Technol., 14: 110-126.

Webb, S.L., Knoche, R. and Dingwell, D.B., 1992. Determination of silicate liquid thermal expansivity using dilatometry and calorimetry. Eur. J. Mineral., 4: 95-104.

Zallen, R., 1983. The Physics of Amorphous Solids. Wiley, New York, N.Y., 304 pp.